ELSEVIER

Journal of Photochemistry and Photobiology A: Chemistry 104 (1997) 59–64

Journal of PHOTOCHEMISTRY AND PHOTOBIOLOGY A:CHEMISTRY

Efficient photoinduced electron transfer between C_{60} and tetrathiafulvalenes studied by nanosecond laser photolysis

Maksudul M. Alam, Akira Watanabe, Osamu Ito *

Institute for Chemical Reaction Science, Tohoku University, Katahira, Aoba-ku, Sendai 980-77, Japan

Received 8 October 1996; accepted 2 January 1997

Abstract

Photoinduced electron transfer between C_{60} and tetrathiafulvalene (TTF) or bis(ethylenedithio)tetrathiafulvalene (BEDT-TTF) in polar and non-polar solvents and their mixtures was investigated by nanosecond laser photolysis/transient absorption spectroscopy in the visible and near-IR regions. The transient absorption bands of the C_{60} triplet ($^{T}C_{60}^{*}$) observed in polar solvents decay on addition of TTF (or BEDT-TTF), accompanied by the appearance of the transient absorption bands of $C_{60}^{\cdot-}$. The yields of $C_{60}^{\cdot-}$ are decreased on addition of O_2, revealing that about 10% of $C_{60}^{\cdot-}$ is produced via the singlet state at donor concentrations of less than 5×10^{-3} M. In benzene, the quenching of $^{T}C_{60}^{*}$ without the appearance of $C_{60}^{\cdot-}$ within the nanosecond laser pulse is attributed to collisional quenching. The quantum efficiencies of $C_{60}^{\cdot-}$ formation via $^{T}C_{60}^{*}$, which were evaluated from the initial [$^{T}C_{60}^{*}$] and maximal [$C_{60}^{\cdot-}$] values, vary with the donor ability and solvent polarity. The forward electron transfer rate constants were evaluated from the decay rates of $^{T}C_{60}^{*}$ (or the rise rates of $C_{60}^{\cdot-}$) after multiplying by the quantum efficiencies. The back electron transfer rates are slowed down in polar solvents. © 1997 Elsevier Science S.A.

Keywords: C_{60}; Electron transfer; Laser photolysis; Tetrathiafulvalene

1. Introduction

The photoinduced electron transfer reactions of fullerenes, such as C_{60} and C_{70}, have been investigated by various methods including time-resolved absorption spectroscopy [1–9]. The initial steps of the electron transfer reactions are dependent on the experimental conditions, such as the donor ability, concentration of the donor and reaction medium. When electron donors form charge transfer complexes with C_{60} (or C_{70}) in the ground state, electron transfer takes place via an exciplex [1,5,6]. In non-polar solvents, the lifetime of the ion radical states is short (less than 300 ps) [1,6], which makes it difficult to observe the ion radicals by the nanosecond laser photolysis technique.

At low donor concentrations in polar solvents, electron transfer takes place via the triplet states of C_{60} and C_{70} ($^{T}C_{60}^{*}$ and $^{T}C_{70}^{*}$) [2,8]. The ion radicals are long lived, up to approximately 50 μs [3]. The relationship between the electron transfer rates and the oxidation potentials of the donor molecules confirms the Rehm–Weller relation [2,8]. For these investigations, the quenching rate constants of $^{T}C_{60}^{*}$ (k_{qT}^{obs}) were set equal to the electron transfer rate constants (k_{et}^{T}), which implies that each electron transfer quantum yield via $^{T}C_{60}^{*}$ is unity. However, the efficiency of electron transfer has not yet been evaluated, because it is necessary to observe both $C_{60}^{\cdot-}$ (or $C_{70}^{\cdot-}$) and $^{T}C_{60}^{*}$ (or $^{T}C_{70}^{*}$) at the same time. Thus we need to detect the formation of the anion radical $C_{60}^{\cdot-}$ (or $C_{70}^{\cdot-}$), which appear in the near-IR region. In this report, we employed nanosecond laser photolysis with a detector with the ability to measure the absorption changes in the near-IR region.

The electron donors tetrathiafulvalene (TTF) and bis(ethylenedithio)tetrathiafulvalene (BEDT-TTF) were used in this study, since they are good electron donors forming charge transfer complexes (or radical ion salts) with various electron acceptors [10–14]. C_{60} has been reported to form a stable radical ion salt with TTF [15,16]. It is interesting to investigate the photoinduced electron transfer in dilute solution, since these systems remain unchanged on light illumination over a long period.

We determined the rate constants of decay of $^{T}C_{60}^{*}$ (k_{qT}^{obs}) and the rate constants of the rise of $C_{60}^{\cdot-}$ ($k_{C_{60}^{\cdot-}}^{obs}$). On combining the quantum yields of electron transfer via $^{T}C_{60}^{*}$ with k_{qT}^{obs} or $k_{C_{60}^{\cdot-}}^{obs}$ we were able to evaluate the electron transfer rate constants via $^{T}C_{60}^{*}$ (k_{et}^{T}). We also examined the effect of the solvent polarity on these quantities. From the effect of O_2 on ion radical formation, the contribution of the singlet states of

* Corresponding author. Tel.: +81 22 217 5608; fax: +81 22 217 5608.

1010-6030/97/$17.00 © 1997 Elsevier Science S.A. All rights reserved
PII S1010-6030(97)00017-8

the fullerenes was also estimated. Information on back electron transfer was also obtained.

2. Experimental details

C_{60} was obtained from Texas Fullerenes Corporation with a purity of 99.9%. Commercially available TTF, BEDT-TTF and solvents were used; benzonitrile and benzene were of high performance liquid chromatography (HPLC) and spectrophotometric grade respectively. C_{60} and TTF (or BEDT-TTF) were dissolved in benzonitrile, benzene or a mixture; the sample solutions were deaerated by bubbling with argon gas before measurement. When the effect of O_2 was investigated, an O_2-saturated solution was produced by O_2 bubbling.

C_{60} was excited by an Nd:YAG laser (Quanta-Ray, GCR-130; full width at half-maximum (FWHM), 6 ns) at 532 nm with a laser power of 5 mJ per pulse. For transient absorption measurements on the nanosecond timescale in the near-IR region, a Ge-APD module (Hamamatsu, C5331-SPL) detector attached to a monochromator was employed, with a pulsed Xe lamp (15 J per pulse, 60 μs FWHM) used as probe light [17]. The response time of the Ge-APD detector of this system was less than 10 ns, which is about the same as the duration of the laser pulse. The output signals from the detectors were recorded with a digitizing oscilloscope and analysed by a personal computer. All experiments were carried out at 23 °C.

The steady state UV–visible absorption spectra were recorded using a Jasco V-570 UV–visible spectrophotometer.

3. Results and discussion

The steady state absorption spectra of C_{60} and TTF in benzonitrile were recorded between 400 and 800 nm as shown in Fig. 1(A). The absorption spectrum of a mixture of C_{60} and TTF in benzonitrile (Fig. 1(B)) is a superimposition of the components, suggesting no apparent interaction at the concentration region employed in the laser photolysis experiments (less than 5 mM) [18,19]. The absorption bands of the components are not appreciably affected by the solvent polarity [19]. In benzene, the absorption spectrum of the mixture is a superimposition of the components, similar to that observed in benzonitrile, suggesting no interaction in non-polar solvents. On laser photolysis at 532 nm, C_{60} only is excited, because of the lack of absorption of TTF at this wavelength.

The laser flash photolysis of C_{60} (0.1 mM) was carried out in the presence of TTF (1.0–6.0 mM) in benzonitrile. Fig. 2 shows the transient absorption spectra in the visible and near-IR regions. A sharp absorption peak at 750 nm, which is observed immediately after the nanosecond laser pulse, is attributed to $^{T}C_{60}^{*}$ [20–31]. With the decay of $^{T}C_{60}^{*}$, absorption bands appear at 950 and 1070 nm, which have been assigned to $C_{60}^{\cdot-}$ in the literature [1,2,24–30]. The decay curve of $^{T}C_{60}^{*}$ at 750 nm and the rise curve of $C_{60}^{\cdot-}$ at 1070 nm are shown in the insets in Fig. 2. The decay and rise profiles obey first-order kinetics, which implies that 1 mM of TTF is in large excess compared with $[^{T}C_{60}^{*}]$. The initial concentration of $^{T}C_{60}^{*}$ is calculated to be about 0.02 mM from the initial absorbance ($A_{T_{C_{60}}^{*}} = 0.3$) and the reported extinction coefficient ($\epsilon_{T_{C_{60}}^{*}} = 1.61 \times 10^{4}\ M^{-1}\ cm^{-1}$) [31]. This implies that the second-order rate constants for quenching of $^{T}C_{60}^{*}$ by TTF (k_{qT}^{obs}) can be obtained from the pseudo-first-order plots of the observed first-order decay rate constants (k_{1st}). After reaching a maximum at about 400 ns, $C_{60}^{\cdot-}$ begins to decay. The absorption band of $TTF^{\cdot+}$ is expected in the wavelength region shorter than 600 nm; thus no absorption band of $TTF^{\cdot+}$ appears in the near-IR region [10].

The rise and decay curves of $C_{60}^{\cdot-}$ in deaerated, aerated and O_2-saturated solutions are shown in Fig. 3. With an increase in the O_2 concentration, the yield of $C_{60}^{\cdot-}$ decreases; about two-thirds of $C_{60}^{\cdot-}$ disappears in aerated solution and 90% of $C_{60}^{\cdot-}$ disappears in O_2-saturated solution. This also confirms that $C_{60}^{\cdot-}$ is mainly formed via $^{T}C_{60}^{*}$. About 10% of $C_{60}^{\cdot-}$ may be produced via the excited singlet state of C_{60} ($^{S}C_{60}^{*}$) or via an exciplex route. The observed electron transfer mechanism for C_{60} is summarized in Scheme 1. The decay rates of $C_{60}^{\cdot-}$ seem to be similar irrespective of the O_2 concentration, indicating that the depletion of $C_{60}^{\cdot-}$ cannot be attributed to a secondary reaction between $C_{60}^{\cdot-}$ and O_2.

In Scheme 1, 10% of the $^{S}C_{60}^{*}$ route implies a ratio of $k_{et}^{S}[TTF]/k_{isc} = 0.1$ for $[TTF] = 1.0$ mM, in which k_{isc}

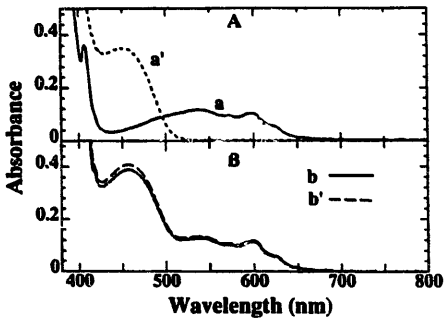

Fig. 1. Steady state absorption spectra. (A) C_{60} (0.1 mM, ———) and TTF (1.0 mM, - - -) spectra. (B) Simulated (b, ———) and observed (b', - - -) spectra of mixture of C_{60} and TTF in benzonitrile.

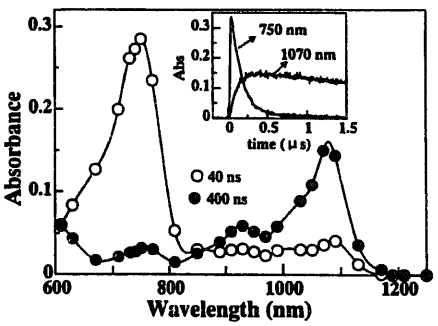

Fig. 2. Transient absorption spectra obtained by 532 nm laser photolysis of C_{60} (0.1 mM) in the presence of TTF (1.0 mM) in deaerated benzonitrile: ○, 40 ns; ●, 400 ns. Inset: time profiles at 750 and 1070 nm.

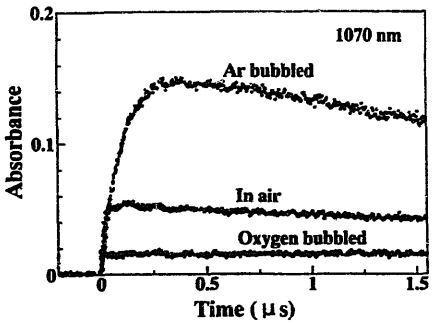

Fig. 3. Rise and decay curves of $C_{60}^{\cdot-}$ in Ar-, air- and O_2-saturated solutions of TTF (1.0 mM).

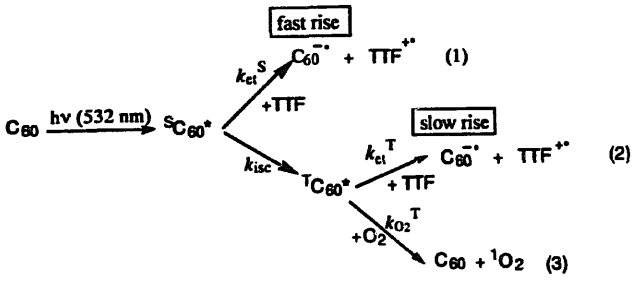

Scheme 1.

denotes the intersystem crossing rate constant. The k_{isc} value for $^{S}C_{60}^{*}$ has been reported to be 1.1×10^{9} s^{-1} [5]; k_{et}^{S} is 1.1×10^{11} M^{-1} s^{-1}, which is about 20 times greater than the diffusion-controlled limit (5.2×10^{9} M^{-1} s^{-1} in benzonitrile), suggesting that electron transfer in $^{S}C_{60}^{*}$ occurs via an exciplex with TTF, but not via collision of free $^{S}C_{60}^{*}$ with TTF.

In the case of C_{60} with BEDT-TTF, similar photoinduced electron transfer behaviour is observed in polar solvents. The formation and rise rates of $C_{60}^{\cdot-}$ at 1070 nm in benzonitrile increase with increasing concentration of BEDT-TTF as shown in Fig. 4. With an increase in [BEDT-TTF], the initial fast rise within the laser pulse seems to increase, suggesting a small contribution of fast electron transfer processes, such as the $^{S}C_{60}^{*}$ and/or exciplex routes. The first-order rate constants can be obtained by curve fitting to the growth of $C_{60}^{\cdot-}$ after subtracting the fast rise part. The slope of the pseudo-first-order plot (inset in Fig. 4) gives the rate constant for the

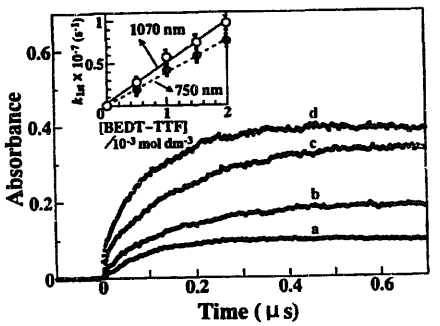

Fig. 4. Rise and decay curves of $C_{60}^{\cdot-}$ at 1070 nm in the presence of BEDT-TTF: (a) 0.5 mM, (b) 1.0 mM, (c) 1.5 mM and (d) 2.0 mM in deaerated benzonitrile. Inset: pseudo-first-order plots of the rise of $C_{60}^{\cdot-}$ and decay of $^{T}C_{60}^{*}$.

rise of $C_{60}^{\cdot-}$ ($k_{C_{60}^{\cdot-}}^{obs}$), which is in agreement with k_{qT}^{obs} within estimation errors. In Table 1, the observed second-order rate constants thus obtained are listed for C_{60} with TTF and BEDT-TTF in benzonitrile. A general relation $k_{qT}^{obs}=k_{C_{60}^{\cdot-}}^{obs}$ can be proven, although $k_{C_{60}^{\cdot-}}^{obs}$ seems to be slightly larger than k_{qT}^{obs} and may include a larger experimental error than k_{qT}^{obs}, because of the initial fast rise of $C_{60}^{\cdot-}$ due to the laser pulse width or scattered light. Thus each k_{qT}^{obs} value is more reliable than $k_{C_{60}^{\cdot-}}^{obs}$.

The efficiency of $C_{60}^{\cdot-}$ formation via $^{T}C_{60}^{*}$ is calculated from the absorbances ($A_{C_{60}^{\cdot-}}$ and $A_{T_{C_{60}}^{\cdot}}$) and extinction coefficients ($\epsilon_{C_{60}^{\cdot-}}$ and $\epsilon_{T_{C_{60}}^{\cdot}}$) as follows: $[C_{60}^{\cdot-}]_{max}/[^{T}C_{60}^{*}]_{max}=(A_{C_{60}^{\cdot-}}/\epsilon_{C_{60}^{\cdot-}})/(A_{T_{C_{60}}^{\cdot}}/\epsilon_{T_{C_{60}}^{\cdot}})$ [9]. On substituting the reported values for $\epsilon_{T_{C_{60}}^{\cdot}}$ and $\epsilon_{C_{60}^{\cdot-}}$ [9,31,32], $[C_{60}^{\cdot-}]_{max}/[^{T}C_{60}^{*}]_{max}$ is plotted against [TTF] as shown in Fig. 5. The $[C_{60}^{\cdot-}]_{max}/[^{T}C_{60}^{*}]_{max}$ value increases with [TTF] and reaches a plateau, which is defined as the quantum yield (Φ_{et}^{T}) of electron transfer via $^{T}C_{60}^{*}$. The Φ_{et}^{T} values are summarized in Table 2. All reaction systems in Table 2 show $\Phi_{et}^{T}<1$. For C_{60}, Φ_{et}^{T} of TTF (approximately 0.75) is slightly greater than that of BEDT-TTF (0.62) in benzonitrile.

For C_{60}–TTF in a 1 : 1 mixture of benzonitrile–benzene, the absorption band of $C_{60}^{\cdot-}$ at 1070 nm appears at the same time as the decay of the absorption band of $^{T}C_{60}^{*}$ at 750 nm, similar to the observations in benzonitrile (Fig. 1). The differences include the faster decay rate of $^{T}C_{60}^{*}$ at 750 nm and the faster rise of $C_{60}^{\cdot-}$ at 1070 nm in the 1 : 1 mixture. The k_{qT}^{obs} values are listed in Table 1; they are greater than those in benzonitrile. In general, it would be anticipated that electron transfer would be accelerated in polar solvents [33]. However, the observed tendency for k_{qT}^{obs} in Table 1 is opposite to that which is expected. This suggests that k_{qT}^{obs} is an apparent value including the collisional deactivation of $^{T}C_{60}^{*}$ by TTF. In order to evaluate the electron transfer rate constant (k_{et}^{T}), it is necessary to obtain Φ_{et}^{T}, since k_{et}^{T} is calculated from k_{qT}^{obs} by multiplying with Φ_{et}^{T} [9]. The Φ_{et}^{T} values in benzene–benzonitrile (1 : 1) are smaller than those in benzonitrile (Table 2). After reaching a maximum, $C_{60}^{\cdot-}$ begins to decay with second-order kinetics, which are faster than those in benzonitrile.

In contrast, in benzene, only the absorption band of $^{T}C_{60}^{*}$ at 750 nm appears, and the absorption band of $C_{60}^{\cdot-}$ is not observed by the nanosecond laser pulse (Fig. 6). Since the increase in the decay rate of $^{T}C_{60}^{*}$ on addition of TTF is observed as shown in the inset, it is confirmed that the quenching of $^{T}C_{60}^{*}$ by TTF takes place without the appearance of $C_{60}^{\cdot-}$. This is attributed to collisional quenching which takes place without electron transfer. The rate constant for collisional quenching, which is referred to as k_{c}^{T}, can be set equal to k_{qT}^{obs} (Table 1). In benzene, Φ_{et}^{T} decreases to zero (Table 2).

For $^{T}C_{60}^{*}$ in the presence of TTF, photoinduced electron transfer and collisional quenching must be taken into consideration as shown in Scheme 2. The relative contributions are changed by the solvent polarity. In Table 2, the Φ_{et}^{T} values increase with increasing solvent polarity; in benzonitrile–benzene (1 : 1), the Φ_{et}^{T} value for each reaction system is

Table 1
Rate constants of $^{T}C_{60}^{*}$ quenching (k_q^T) and $C_{60}^{\cdot-}$ formation (k_{C60}) for TTF and BEDT-TTF in benzonitrile, benzene and a 1 : 1 mixture[a]

Solvent[b]	TTF		BEDT-TTF	
	k_q^T ($M^{-1}s^{-1}$)	k_{C60} ($M^{-1}s^{-1}$)	k_q^T ($M^{-1}s^{-1}$)	k_{C60} ($M^{-1}s^{-1}$)
BN	5.0×10^9	6.1×10^9	3.8×10^9	4.9×10^9
1 : 1	8.2×10^9	1.2×10^{10}	5.3×10^9	8.3×10^9
BZ	9.9×10^9	–[c]	5.9×10^9	–[c]

[a]Each rate constant contains experimental and estimation errors of 10%.
[b]BN, benzonitrile; BZ, benzene; 1 : 1, mixture of BN and BZ.
[c]$C_{60}^{\cdot-}$ radical anion was not observed in benzene.

Table 2
Observed quantum yield (Φ_{et}^T)[a] of $C_{60}^{\cdot-}$ formation via $^{T}C_{60}^{*}$ and calculated k_{et}^T and k_c^T values for TTF and BEDT-TTF[b]

Solvent	TTF			BEDT-TTF		
	Φ_{et}^T	k_{et}^T ($M^{-1}s^{-1}$)	k_c^T ($M^{-1}s^{-1}$)	Φ_{et}^T	k_{et}^T ($M^{-1}s^{-1}$)	k_c^T ($M^{-1}s^{-1}$)
BN	0.75	3.8×10^9	1.2×10^9	0.62	2.4×10^9	1.4×10^9
(1 : 1)	0.37	3.0×10^9	5.2×10^9	0.25	1.3×10^9	4.0×10^9
BZ	0.00	0	9.9×10^9	0.00	0	5.9×10^9

[a]$[C_{60}^{\cdot-}]_{max}/[^{T}C_{60}^{*}]_{initial}$ was evaluated using the observed absorbances and reported ϵ values (ϵ of $^{T}C_{60}^{*}$ at 750 nm, 16 100 $M^{-1}cm^{-1}$ [31]; ϵ of $C_{60}^{\cdot-}$ at 1070 nm, 12 100 $M^{-1}cm^{-1}$ [32]). When ϵ_{C60} = 18 300 $mol^{-1}dm^3cm^{-1}$ is employed [9], each Φ_{et}^T becomes about 1/1.5.
[b]Each k_{et}^T value from $\Phi_{et}^T k_q^T$ is about 10% smaller than that from $\Phi_{et}^T k_{C60}$, which is within experimental error.

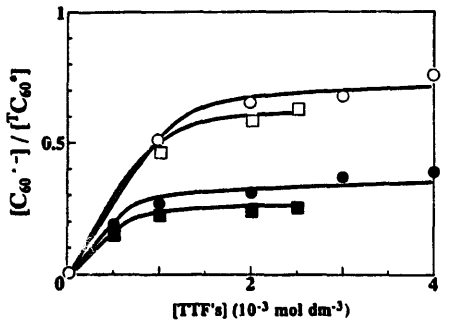

Fig. 5. Dependence of $C_{60}^{\cdot-}$ formation efficiency via $^{T}C_{60}^{*}$ on [TTF]: TTF (○) and BEDT-TTF (□) in benzonitrile; TTF (●) and BEDT-TTF (■) in benzonitrile–benzene (1 : 1).

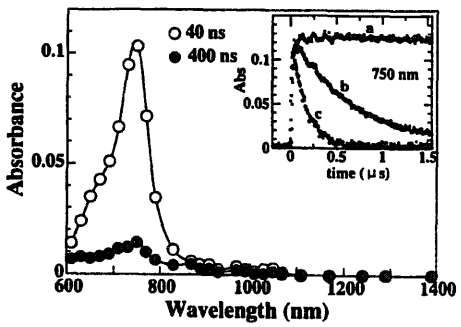

Fig. 6. Transient absorption spectra obtained by 532 nm laser flash photolysis of C_{60} (0.1 mM) in the presence of BEDT-TTF (1.0 mM) in deaerated benzene: ○, 40 ns; ●, 400 ns. Inset: decay profiles of $^{T}C_{60}^{*}$ at 750 nm in the presence of BEDT-TTF: (a) 0.0 mM; (b) 0.2 mM; (c) 1.0 mM.

about one-half of the corresponding value in benzonitrile. This is reasonably interpreted by the facile ionization of the encounter complex in the polar solvent [33].

In Table 1, $k_{qT}^{obs} = k_{C60}^{obs}$ is valid in benzonitrile within experimental and estimation errors, but $k_{qT}^{obs} < k_{C60}^{obs}$ in benzene–benzonitrile (1 : 1). In terms of the laser pulse width and curve-fitting technique, k_{C60}^{obs} is less reliable than k_{qT}^{obs}, which was chosen for the calculation of k_{et}^T.

From Scheme 2, $\Phi_{et}^T = k_{et}^T/(k_{et}^T + k_c^T)$ was derived; thus $k_{et}^T = \Phi_{et}^T(k_{et}^T + k_c^T) = \Phi_{et}^T k_{qT}^{obs}$. The k_{et}^T values calculated from k_{qT}^{obs} by multiplying by Φ_{et}^T are listed in Table 2. From the Rehm–Weller equation [34], the free energy change (ΔG_0) can be calculated to be −70.45 kJ mol^{-1} for TTF and −52.11 kJ mol^{-1} for BEDT-TTF in benzonitrile by employing the T_1 energy level of $^{T}C_{60}^{*}$ (1.53 eV) [35], the reduction potential of C_{60} (−0.51 eV) [36–38], the oxidation potentials of the electron donors (0.35 eV for TTF and 0.54 eV for BEDT-TTF) [10,11,13] and the Coulomb energy (0.06 eV) [8]. These negative ΔG_0 values anticipate that k_{et}^T is close to

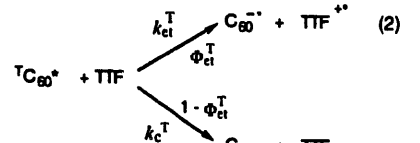

Scheme 2.

the diffusion-controlled limit (i.e. 5.2×10^9 $M^{-1}s^{-1}$ in benzonitrile). The evaluated k_{et}^T values (Table 2), however, are slightly less than the diffusion-controlled limit. Comparing k_{et}^T for TTF with that for BEDT-TTF, it can be seen that the former is greater than the latter, which is in accord with the order of the calculated ΔG_0 values, i.e. the more negative the ΔG_0 value, the greater the k_{et}^T value. k_{et}^T is small in less polar solvents, which is a reasonable tendency confirming the solvation stabilization of the ion radicals in polar solvents. In contrast, the opposite tendency is found for $k_c^T = (1 - \Phi_{et}^T)k_{qT}^{obs}$, which is also reasonable because collisional quench-

Table 3
Rate constants for back electron transfer (k_{bet}) for TTF and BEDT-TTF in benzonitrile, benzene and a 1 : 1 mixture

Solvent	TTF		BEDT-TTF	
	$k_{bet}/\epsilon_{C_{60}^{\cdot-}}$ (s^{-1} cm^{-1})	k_{bet} (M^{-1} s^{-1})	$k_{bet}/\epsilon_{C_{60}^{\cdot-}}$ (s^{-1} cm^{-1})	k_{bet} (M^{-1} s^{-1})
BN	7.9×10^{5}	9.5×10^{9}[a]	5.3×10^{5}	6.4×10^{9}[a]
1 : 1	1.9×10^{6}	2.3×10^{10}[a]	1.8×10^{6}	2.2×10^{10}[a]
BZ	_[b]	_[b]	_[b]	_[b]

[a] $\epsilon_{C_{60}^{\cdot-}}$ = 12 100 M^{-1} cm^{-1} at 1070 nm [32].
[b] The C_{60} radical anion was not observed in benzene.

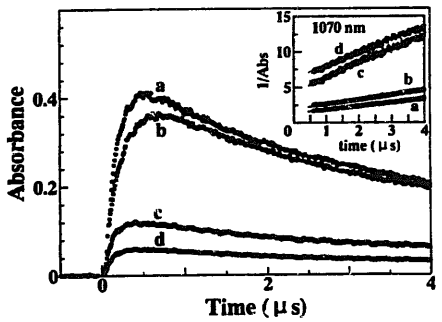

Fig. 7. Rise and decay curves of $C_{60}^{\cdot-}$ at 1070 nm for TTF (a) and BEDT-TTF (b) in benzonitrile and TTF (c) and BEDT-TTF (d) in benzonitrile–benzene (1 : 1). Inset: second-order plots for the decay of $C_{60}^{\cdot-}$.

ing would be expected to take place favourably in less polar solvents.

In benzene, we observed only $^{T}C_{60}^{*}$ without $C_{60}^{\cdot-}$ formation; if electron transfer takes place in less than a nanosecond, forming a contact ion pair which quickly returns to the neutral molecules, $^{T}C_{60}^{*}$ will not be observed on a timescale of 500–1000 ns. Our observation of $^{T}C_{60}^{*}$ in benzene suggests that electron transfer does not take place at an early stage, because of the lack of a strong charge transfer interaction, the low concentration of electron donor employed in this study and the observed large k_c^{T} values with TTFs containing sulphur atoms.

In Scheme 1, $k_{O_2}[O_2]$ in aerated benzonitrile solution ($[O_2]$ = 2.0 mM) is comparable with $k_{et}[TTF]$ at 1.0 mM, because appreciable $C_{60}^{\cdot-}$ is observed (Fig. 3). Since k_{O_2} is reported to be 1.9×10^{9} M^{-1} s^{-1} [31], k_{et} should be about 4×10^{9} M^{-1} s^{-1}, which is in good agreement with the result in this study (Table 2).

After reaching a maximum, $C_{60}^{\cdot-}$ begins to decay as shown in Fig. 7. From the slopes of the second-order plots shown in the inset, the ratio of the second-order rate constant for back electron transfer (k_{bet}) to $\epsilon_{C_{60}^{\cdot-}}$ can be obtained. On substituting $\epsilon_{C_{60}^{\cdot-}}$ (12 100 M^{-1} cm^{-1} at 1070 nm in benzonitrile) [32], the k_{bet} values are determined as summarized in Table 3.

$$C_{60}^{\cdot-} + TTF^{\cdot+} \xrightarrow{k_{bet}} C_{60} + TTF \quad (5)$$

When 50% benzene is added to benzonitrile, the k_{bet} values increase about two- or three-fold assuming the same ϵ value for $C_{60}^{\cdot-}$ as that in benzonitrile. With decreasing solvent polarity, back electron transfer rates tend to increase, suggesting that ion radicals in less polar solvents exist as more tightly combined ion pairs.

By repeated exposure with the 532 nm laser of C_{60}–TTF, the steady state absorption spectra remain unchanged up to 10 000 shots with a laser power of 10 mJ. Thus the system is photochemically very stable. When the solution used for laser photolysis is kept cool in the dark, black whiskers attributed to $(C_{60})^{\cdot-}(TTF)_2^{+}$ are observed [15,16], indicating that laser irradiation stimulates the growth of long whiskers. Further study is in progress.

4. Conclusions

By observing directly the rise of $C_{60}^{\cdot-}$ in addition to the decay of $^{T}C_{60}^{*}$ at the same time, electron transfer via $^{T}C_{60}^{*}$ was confirmed, which was also supported by the decrease in $C_{60}^{\cdot-}$ on addition of O_2. The electron transfer rates were evaluated by multiplying the observed quantum efficiency by the decay rate of $^{T}C_{60}^{*}$. With a variation in the solvent polarity, the change in the electron transfer rate was interpreted well. A solvent polarity dependence of the back electron transfer rate was also revealed.

Acknowledgements

This work was partially supported by Grants-in-Aid on Priority-Area-Research on "Photoreaction Dynamics" (No. 08218207) and "Functionally Graded Material" (No. 0824326) from the Ministry of Education, Science, Sports and Culture. The authors wish to thank Professor H. Kokubun (Aomori University) for useful comments.

References

[1] R. Sension, A.Z. Szarka, G.R. Smith, R.M. Hochstrasser, Chem. Phys. Lett. 185 (1991) 179.
[2] J.W. Arbogast, C.S. Foote, M. Kao, J. Am. Chem. Soc. 114 (1992) 2277.
[3] L. Biczok, H. Linschitz, Chem. Phys. Lett. 195 (1992) 339.
[4] S. Nonell, J.W. Arbogast, C.S. Foote, J. Phys. Chem. 96 (1992) 4169.
[5] D.K. Palit, H.N. Ghosh, H. Pal, A.V. Sapre, J.P. Mittal, R. Seshadri, C.N.R. Rao, Chem. Phys. Lett. 198 (1992) 113.

[6] H. Ghosh, H. Pal, A.V. Sapre, J.P. Mittal, J. Am. Chem. Soc. 115 (1993) 11 722.
[7] D.M. Guldi, H. Hungerbuhler, E. Janata, K.-D. Asmus, J. Chem. Soc., Chem. Commun. (1993) 84.
[8] T. Osaki, Y. Tai, M. Tazawa, S. Tanemura, K. Inukawa, K. Ishiguro, Y. Sawaki, Y. Saito, H. Shinohara, H. Nagashima, Chem. Lett. (1993) 789.
[9] C.A. Steren, H. von Willigen, L. Biczok, N. Gupta, H. Linschitz, J. Phys. Chem. 100 (1996) 8920.
[10] S. Hunig, G. Kiesslich, H. Quast, D. Scheutzow, Liebigs Ann. Chem. 766 (1973) 310.
[11] K. Nakatsuji, M. Nakatsuak, H. Yamochi, I. Murata, S. Harada, N. Kasai, K. Yamamura, J. Tanaka, G. Saito, T. Enoki, H. Inokuchi, Bull. Chem. Soc. Jpn. 59 (1986) 207.
[12] D.L. Lichtenberger, R.L. Johnston, K. Hinkelmann, T. Suzuki, F. Wudl, J. Am. Chem. Soc. 112 (1990) 3302.
[13] G. Grampp, A. Kapturkiewicz, W. Jaenicke, Ber. Bunsenges. Phys. Chem. 94 (1990) 439.
[14] M.R. Bryce, Chem. Rev. 20 (1991) 355.
[15] P. Bowmar, M. Kurmoo, M.A. Green, F.P. Pratt, W. Hayes, P. Day, K. Kikuchi, J. Phys.; Condensed Matter 5 (1993) 2739.
[16] A. Izuoka, T. Tachikawa, T. Sugawara, Y. Suzuki, M. Konno, Y. Saito, H. Shinohara, J. Chem. Soc., Chem. Commun. (1992) 1472.
[17] A. Watanabe, O. Ito, J. Phys. Chem. 98 (1994) 7736.
[18] H. Ajie, M.M. Alvarez, S.J. Anz, R.D. Beck, F. Diederich, K. Fostiropoulos, D.R. Hiffman, W. Kratschmer, Y. Rubin, K.E. Schriver, D. Sensharma, R.L. Whetten, J. Phys. Chem. 94 (1990) 8630.
[19] S.H. Gallagher, R.S. Armstrong, P.A. Lay, C.A. Reed, J. Phys. Chem. 99 (1995) 5817.
[20] Y. Kajii, T. Nakagawa, S. Suzuki, Y. Achiba, K. Obi, K. Shibuya, Chem. Phys. Lett. 181 (1991) 100.
[21] R.J. Sension, C.M. Phillips, A.Z. Szarka, W.J. Romanow, A.R. Macghie, J.P. McCauley, A.B. Smith III Jr., R.M. Hochstrasser, J. Phys. Chem. 95 (1991) 6075.
[22] T. Ebbesen, K. Tanigaki, S. Kuroshima, Chem. Phys. Lett. 181 (1991) 501.
[23] N.M. Dimitrijevic, P.V. Kamat, J. Phys. Chem. 96 (1992) 4811.
[24] T. Kato, T. Kodama, T. Shida, T. Nakagawa, Y. Matsui, S. Suzuki, H. Shiromaru, K. Yamauchi, Y. Achiba, Chem. Phys. Lett. 180 (1991) 446.
[25] M.A. Greaney, S.M. Gorun, J. Phys. Chem. 95 (1991) 7142.
[26] Z. Gasyna, L. Andrews, P.N. Schatz, J. Phys. Chem. 96 (1992) 1525.
[27] D.M. Guldi, H. Hungerbuhler, E. Janata, K.-D. Asmus, J. Phys. Chem. 97 (1993) 11 258.
[28] O. Ito, Y. Sasaki, Y. Yoshikawa, A. Watanabe, J. Phys. Chem. 99 (1995) 9838.
[29] Y. Sasaki, Y. Yoshikawa, A. Watanabe, O. Ito, J. Chem. Soc., Faraday Trans. 91 (1995) 2287.
[30] A. Watanabe, O. Ito, K. Mochida, Organometallics 14 (1995) 4281.
[31] J.W. Arbogast, A.P. Darmanyan, C.S. Foote, Y. Rubin, F.N. Diederich, M.M. Alvarez, S.J. Anz, R.L. Whetten, J. Phys. Chem. 95 (1991) 11.
[32] G.A. Heath, J.E. McGrady, R.L. Martin, J. Chem. Soc., Chem. Commun. (1992) 1272.
[33] M. Mataga, Adv. Chem. 228 (1991) 6.
[34] D. Rehm, A. Weller, Isr. J. Chem. 8 (1970) 259.
[35] R.R. Hung, J.J. Grabowski, J. Phys. Chem. 95 (1991) 6073.
[36] R.E. Haufler, J. Conceicao, L.P.F. Chibante, Y. Chai, N.E. Byrne, S. Flanagan, M.M. Haley, S.C. O'Brien, C. Pan, Z. Xiao, W.E. Billups, M.A. Ciufolini, R.H. Hauge, J.L. Margrave, L.J. Wilson, R.F. Curl, R.E. Smally, J. Phys. Chem. 94 (1990) 8634.
[37] P.M. Allemand, A. Koch, F. Wudl, Y. Rubin, F. Diederich, M.M. Alvarez, S.J. Anz, R.L. Whetten, J. Am. Chem. Soc. 113 (1991) 1050.
[38] D. Dubois, K.M. Kadish, S. Flanagan, R.E. Haufler, L.P.F. Chibante, L.J. Wilson, J. Am. Chem. Soc. 113 (1991) 4364.